Available online at www.sciencedirect.com
ScienceDirect
Catalysis Today 131 (2008) 305–313
CATALYSIS TODAY
www.elsevier.com/locate/cattod

Selective catalytic reduction of NO by C_3H_8 over CoO_x/Al_2O_3: An investigation of structure–activity relationships

Chuanhua He [a,1], Martin Paulus [a], Wei Chu [b], Josef Find [c], Julius A. Nickl [c], Klaus Köhler [a,*]

[a] Department of Chemistry, Technische Universität München, Lichtenbergstraße 4, D-85747 Garching, Germany
[b] Chemical Engineering School of Sichuan University, 610065 Chengdu, PR China
[c] Gesellschaft für Werkstoffprüfung mbH, Georg-Wimmer-Ring 25, D-85604 Zorneding, Germany

Available online 26 November 2007

Abstract

A series of CoO_x/Al_2O_3 catalysts was prepared, characterized, and applied for the selective catalytic reduction (SCR) of NO by C_3H_8. The results of XRD, UV–vis, IR, Far-IR and ESR characterizations of the catalysts suggest that the predominant oxidation state of cobalt species is +2 for the catalysts with low cobalt loading ($\leq$2 mol%) and for the catalysts with 4 mol% cobalt loading prepared by sol–gel and co-precipitation. Co_3O_4 crystallites or agglomerates are the predominant species in the catalysts with high cobalt loading prepared by incipient wetness impregnation and solid dispersion. An optimized CoO_x/Al_2O_3 catalyst shows high activity in SCR of NO by C_3H_8 (100% conversion of NO at 723 K, GHSV: 10,000 h^{-1}). The activity of the selective catalytic reduction of NO by C_3H_8 increases with the increase of cobalt–alumina interactions in the catalysts. The influences of cobalt loading and catalyst preparation method on the catalytic performance suggest that tiny $CoAl_2O_4$ crystallites highly dispersed on alumina are responsible for the efficient catalytic reduction of NO, whereas Co_3O_4 crystallites catalyze the combustion of C_3H_8 only.

Keywords: Selective catalytic reduction; Nitrogen oxides; $DeNO_x$; Propane; Cobalt; Alumina; Far-IR; ESR

1. Introduction

Selective catalytic reduction (SCR) of nitrogen oxides (NO_x) by hydrocarbons or oxygenated molecules in an oxidizing atmosphere is a promising method to remove NO_x from lean burn and diesel engine exhaust and could be an interesting cheaper alternative to ammonia SCR, e.g., for power stations [1–6]. Although the first catalysts reported and many studies focused on SCR of NO by hydrocarbons are related to zeolite or metal ion exchanged zeolite catalysts [7–17], metal oxide or supported metal oxide catalysts are probably the best candidates for this reaction due to their superior hydrothermal stability and sulphur resistance [18–27]. Among the supported metal oxides, CoO_x/Al_2O_3 is a promising candidate for the practical application because of its high stability and activity for NO_x reduction even in the presence of water and an excess of oxygen [26,27]. The activity of CoO_x/Al_2O_3 in the SCR of NO by hydrocarbons is strongly dependent on the precursor of cobalt, the cobalt loading and the preparation procedures [26–30].

Yan et al. [27] and Horiuchi et al. [28] investigated the effect of cobalt loading, calcination temperature and the source of alumina on the surface properties and catalytic performance of Co/Al_2O_3 in SCR of NO by C_3H_6. The authors concluded that octahedral Co^{2+} ions are responsible for the reduction of NO, Co_3O_4 particles or clusters only catalyze the combustion of hydrocarbons and Co^{2+} ions in $CoAl_2O_4$ are inactive. Hamada et al. [29] studied the effect of transition metal additives on the catalytic performance of silica and alumina in the SCR of NO by propane and demonstrated that metal-alumina catalysts containing metal aluminates showed high activity at low temperatures. Nanba et al. [30] investigated the effect of catalyst preparation procedure and calcination temperature on the catalytic

* Corresponding author at: Department of Chemistry, Inorganic Chemistry, Technische Universität München, Lichtenbergstraße 4, D-85747 Garching, Germany. Fax: +49 89 289 13183.
E-mail address: klaus.koehler@ch.tum.de (K. Köhler).
[1] Present address: Degussa (SEA) Pte Ltd., 1 Pesek Road, Jurong Island, Singapore 627833.

0920-5861/$ – see front matter © 2007 Elsevier B.V. All rights reserved.
doi:10.1016/j.cattod.2007.10.024

properties of Co/Al_2O_3 in the SCR of NO by C_3H_6 and proposed that highly dispersed $CoAl_2O_4$ crystallites on alumina are the active centers of NO reduction. More recently, Kung and Kung [18] studied structure–activity relationships in the SCR of NO by C_3H_6 over various alumina supported catalysts and suggested that the metal ion–support interactions, varying with the concentration of active species, nature of support and preparation methods, may markedly effect the surface properties and thus the overall catalytic activity. To elucidate the active centers and the structure–activity relationships of CoO_x/Al_2O_3 in SCR of NO by hydrocarbons, it is important to determine the chemical composition and the surface structure of the CoO_x/Al_2O_3 catalysts as well as to relate their structure and catalytic properties in the SCR reaction. Far-IR and ESR are among the most important technologies to determine the chemical valence and the chemical environment of transient metal species. However, few detailed investigations on the characterization of cobalt–alumina system using Far-IR and ESR are reported.

In this paper, the degrees of cobalt dispersion and cobalt–alumina interactions are adjusted by varying cobalt loading and catalyst preparation method. The catalytic properties of CoO_x/Al_2O_3 catalysts in SCR of NO by C_3H_8 are investigated extensively (conversions as function of various temperatures, detailed selectivity based on complete nitrogen and carbon balance). XRD, UV–vis, Far-IR and ESR are carried out to characterize the prepared catalysts. Emphases are placed on the Far-IR and ESR characterization. On the basis of the catalyst characterization and their catalytic performance, the structure–activity relationships of CoO_x/Al_2O_3 in SCR of NO by propane are discussed.

2. Experimental details

2.1. Catalyst preparation

The CoO_x/Al_2O_3 catalysts applied in this study were prepared using four different methods: co-precipitation, sol–gel, incipient wetness impregnation and solid dispersion:

(1) Co-precipitation method: aluminum nitrate ($Al(NO_3)_3 \cdot 9H_2O$, Merck, >99%) and cobalt nitrate ($Co(NO_3)_2$, Merck, >99%) were dissolved in deionized water to form a mixed solution, then the precipitation was performed using ammonium hydroxide. The precipitate mixture was filtered. The obtained cake was dried at 393 K over night and calcined at 723 K for 4 h in static air.
(2) Sol–gel method: aluminum(III) tri-isopropoxide (Merck, >98%) was dissolved in a certain amount of ethanol. After stirring for 4 h at 78 °C (boiling point of ethanol), distilled water was added and a liquid sol was formed. The sol system was vigorously stirred at 78 °C for 30 min. Then an aqueous solution of cobalt nitrate was added dropwise under continuous stirring. The resulting wet gels were aged at room temperature for 24 h, followed by evaporating the remaining solvents at 363 K and calcined at 723 K for 4 h in static air.
(3) Incipient wetness impregnation: a certain amount of γ-Al_2O_3 (deliverer: Sasol, BET specific surface area: 198 m^2/g) was soaked into a solution of cobalt nitrate in excess of water, kept at room temperature for 2 h with frequent stirring. Then, the water was removed by evaporation under reduced pressure. The sample precursor obtained was dried at 393 K over night and calcined at 723 K for 4 h in static air. The catalysts with 0.5%, 1%, 2% and 8% cobalt in mole were also prepared by this method.
(4) Solid dispersion method: cobalt(II) nitrate and γ-Al_2O_3 were ball milled together and treated at 303 K for 72 h, then calcined at 723 K for 4 h in static air.

The obtained catalysts were marked as CP*x*, SG*x*, IW*x* and SD*x* for the samples prepared by co-precipitation, sol–gel, incipient wetness impregnation and solid dispersion, respectively. Here the first two capital letters are the abbreviation of the preparation method; *x* is the cobalt loading in mol percent which was measured by atomic absorption spectroscopy analysis after dissolution in nitric acid. The specific surface area of the prepared catalysts was measured using an ASAP 2000 apparatus. Before the measurements, the samples were degassed at 523 K for 15 h in an outgassing station of the adsorption apparatus. The full adsorption–desorption isotherm was obtained at 77 K using the Brunauer–Emmett–Teller (BET) method at various relative pressures (five points in the region $0.05 < P/P_0 < 0.3$; nitrogen molecular cross-section area = 16.2 $Å^2$). The cobalt loading, BET specific surface area and the color of the prepared catalysts are listed in Table 1.

Table 1
Cobalt loading and surface area of the catalysts

Code	Preparation method	Cobalt loading (mol%)	Surface area (m^2/g)	Color
Al_2O_3	–	0	200	White
IW05	Incipient wetness impregnation	0.5	197	Pale blue
IW1	Incipient wetness impregnation	1.0	200	Pale blue
IW2	Incipient wetness impregnation	2.0	196	Blue
IW4	Incipient wetness impregnation	4.0	196	Green
IW8	Incipient wetness impregnation	8.0	190	Dark green
SD4	Solid dispersion	4.0	181	Dark green
SG4	Sol–gel	4.0	220	Blue
CP4	Co-precipitation	3.9	217	Blue

2.2. Catalyst characterization

2.2.1. X-ray diffraction

The structures of the phases were determined for finely crushed catalysts in a *Philips PW170* diffractometer using Cu Kα radiation. A continuous scan mode was used to collect 2θ data from 10° to 80° with a 0.02 sampling pitch and a 4°/min scan rate. X-ray tube voltage and current were set at 40 kV and 30 mA, respectively.

2.2.2. UV–vis spectroscopy

UV–vis spectra were measured using UV-Vis spectrometer (*PERKIN ELMER Lambda 9*) in a diffuse reflectance mode.

2.2.3. IR and Far-IR spectroscopy

The catalyst samples were characterized by FT-IR spectroscopy in an *FTS 575C* spectrometer (*BIO-RAD*), using potassium bromide (KBr) pellets (1 mg sample mixed with 125 mg KBr for each pellet). Thirty-two scans with a resolution of 2 cm^{-1} were performed for each spectrum. For Far-IR, 1 mg sample was well mixed with polyethylene and pressed into a pellet. The spectra were recorded by 256 scans with a resolution of 4 cm^{-1}.

2.2.4. ESR spectroscopy

ESR spectra were recorded on a *JEOL JES-RE2X* spectrometer at X-band frequency at $T = 130$ K. The spectra were measured at a microwave frequency of ca. 9.05 GHz with a microwave power of 5 mW, with modulation amplitude of 0.4 mT, sweep time 4 min, sweep width 100 mT, time constant 0.1 s and a modulation frequency of 100 kHz.

2.3. Catalytic activity measurements

The catalytic activity was evaluated by using a fixed bed-flow micro-reactor. The reaction gas mixture consisted of 1000 ppm NO, 1000 ppm C_3H_8 and 10% O_2 (Helium as balance gas). The gas flow rate GHSV is 10,000 h^{-1}. The analysis of feed gas and products was carried out with a mass spectrometer, a CLD NO_x analyzer, a NDIR CO analyzer and a gas micro chromatograph (GC) with a thermal conductivity detector and Porapack Q and molecular sieve A as separation columns. The catalytic activity was evaluated in terms of NO conversion to N_2, C_3H_8 conversion to CO_x (CO + CO_2) and the NO competitiveness factor (NOCF). The formation of N_2O and CO was found negligible in the present work.

3. Results and discussion

3.1. Catalyst characterization

3.1.1. XRD characterization

Fig. 1 shows the XRD patterns of γ-Al_2O_3 and CoO_x/Al_2O_3 prepared by incipient wetness impregnation. A weak reflex centered at 37.1° and two broad reflexes at 45.5° and 67.0° are observed in the XRD pattern of pure alumina. After impregnation of cobalt onto the surface of alumina, a new sharp reflex at 38.6° corresponding to $CoAl_2O_4$ or Co_3O_4 crystallites is observed in the XRD patterns of IW05 and IW1. However, the reflexes at $2\theta = 31.5°$, 45.5° and 65.7° corresponding to Co_3O_4 [31] are not observed in these two XRD patterns. These results suggest that the reflexes at 38.6° in the XRD patterns of IW05 and IW1 could result from $CoAl_2O_4$. Besides the reflexes characteristic of γ-Al_2O_3 and the reflex at 38.6°, new reflexes at $2\theta = 31.5°$, 45.5° and 65.7° corresponding to Co_3O_4 crystallites are observed in the XRD pattern of IW8. This result implies that Co_3O_4 is formed in IW8.

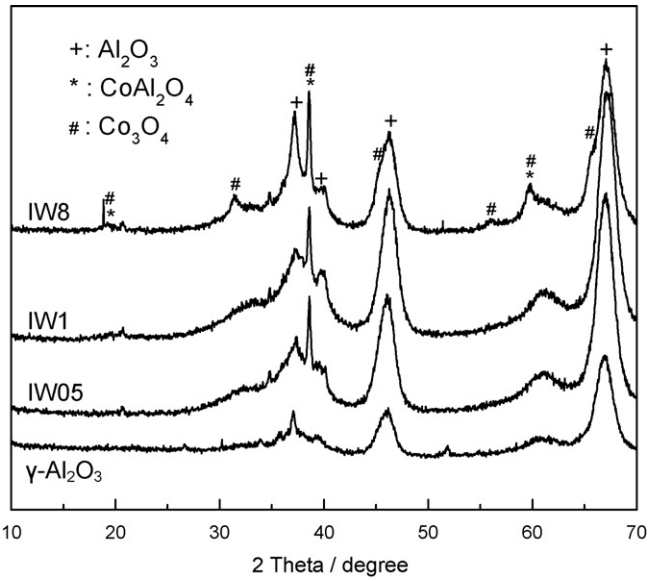

Fig. 1. XRD patterns of CoO_x/γ-Al_2O_3 catalysts with various Co loadings. (*) Co_3O_4; (#) $CoAl_2O_4$ and (+) γ-Al_2O_3.

Fig. 2 shows the XRD patterns of CoO_x/Al_2O_3 prepared by different methods. The XRD pattern of the catalysts prepared by sol–gel (SG4) is similar to pure γ-Al_2O_3, indicating that

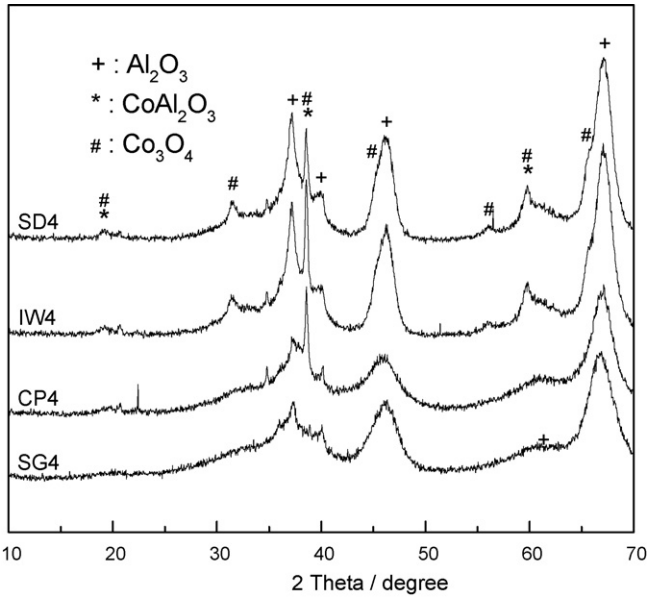

Fig. 2. XRD patterns of 4 mol% CoO_x/γ-Al_2O_3 catalysts prepared by different methods. (*) Co_3O_4; (#) $CoAl_2O_4$ and (+) γ-Al_2O_3.

cobalt species are highly dispersed in the catalysts and new phases are not formed in this sample. In the XRD patterns of CP4, a new reflex at 38.6° corresponding to $CoAl_2O_4$ is observed, suggesting that small $CoAl_2O_4$ crystallites are formed in this catalyst. Reflexes at $2\theta = 31.5°$, 45.5° and 65.7°, corresponding to Co_3O_4 crystallites are observed in the XRD patterns of the catalysts prepared by incipient wetness impregnation (IW4) and solid dispersion (SD4). This suggests that the Co_3O_4 crystallites are formed in the IW4 and SD4 samples. Note the identical cobalt loading and calcination temperatures of these catalysts, the difference in the catalyst structures must result from different cobalt–alumina interactions that varied with the catalyst preparation method.

3.1.2. UV–vis spectroscopy

Fig. 3 shows the effect of cobalt loading and preparation method on the UV–vis spectra of chosen CoO_x/Al_2O_3 catalysts. In the spectra of IW1, IW2, a triplet of bands at 543 nm, 580 nm and 626 nm are observed. Jacono et al. [32] investigated the Uv–vis spectra of Co/Al_2O_3 and $CoMo/Al_2O_3$, the authors attribute the triplet of bands at 16050 cm^{-1}, 17279 cm^{-1} and 18300 cm^{-1} (corresponding to 623 nm, 579 nm and 546 nm, respectively) to the transitions of $^4A_2 \rightarrow {}^4T_1(^4P)$ of the tetrahedral Co^{2+} ions in $CoAl_2O_4$. Therefore, the triplet of bands at 543 nm, 580 nm and 626 nm observed in the spectra of IW1 and IW2 can be assigned to $^4A_2 \rightarrow {}^4T_1(^4P)$ transitions of the tetrahedral Co^{2+} ions in the compound $CoAl_2O_4$. In the spectrum of IW4, the triplet band observed in IW1 and IW2 is disappeared while a broad hump at 550–800 nm is observed. This implies that cobalt oxide species are conglomerated and the formation of $CoAl_2O_4$ is hindered with increasing cobalt loading.

Fig. 3 also demonstrates that the UV–vis spectra of the 4 mol% CoO_x/Al_2O_3 catalysts vary with the preparation method. Identical to spectrum of IW4, a broad hump at 550–800 nm is observed in the spectrum of SD4. This demonstrates that the properties of these two catalysts differ from other chosen catalysts (IW1, CP4 and SG4). In the spectra of CP4 and SG4, again a triplet of bands at 543 nm, 580 nm and 626 nm characteristic of tetrahedral Co^{2+} of $CoAl_2O_4$ is observed. This indicates that cobalt is penetrated into the support matrix and reacted with alumina forming $CoAl_2O_4$ species. A small shoulder at 480 nm ($^4T_{1g}(F) \rightarrow {}^4T_{1g}(P)$) characteristic of octahedral Co^{2+} is detected in the spectra of IW1, IW2 and SG4 [27,33,34], suggesting that octahedral Co^{2+} species are formed in these catalysts. The difference in catalyst structure is also reflected by the color of the catalysts. The catalysts prepared by incipient wetness impregnation, IW1, IW2, IW4 and IW8, are pale blue, bright blue, green and dark green, respectively. In comparison IW4, SD4 are dark green, SG4 and CP4 are blue.

3.1.3. Infrared and Far-Infrared spectroscopy

Infrared and Far-infrared spectra of the catalysts studied in this work were recorded in order to study the structure of CoO_x/Al_2O_3 catalysts. Fig. 4 shows the infrared and Far-infrared spectra of Co_3O_4, $CoAl_2O_4$ and Al_2O_3. In all spectra, two bands characteristic of adsorbed water (1631 cm^{-1}) and carbonate (1384 cm^{-1}) are observed, resulting from the exposure of the samples to air. Double bands at 663 cm^{-1} and 568 cm^{-1}, observed in the spectrum of Co_3O_4, can be assigned to Co–O stretching vibration of cubic spinel Co_3O_4 [35,36]. In the spectrum of $CoAl_2O_4$, two bands centered at 772 cm^{-1} and 676 cm^{-1} are observed, which are assigned to the vibration of normal spinel $CoAl_2O_4$ containing AlO_6 and $Co^{2+}O_4$ groups [37,38]. Pure alumina exhibits two broad bands between 900 cm^{-1} and 500 cm^{-1}. In the Far-IR region, two bands centered at 390 cm^{-1} and 218 cm^{-1} are observed in the spectrum of Co_3O_4, while a broad band at 321 cm^{-1} is observed in the spectrum of Al_2O_3.

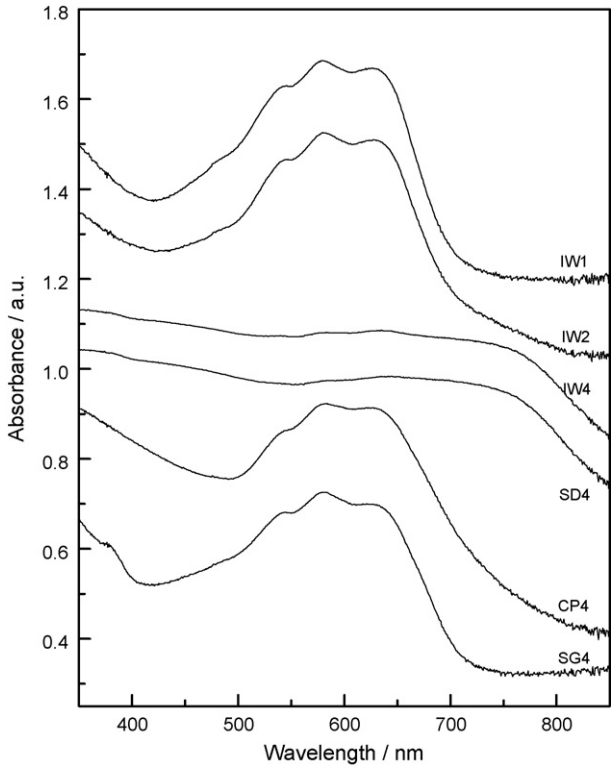

Fig. 3. UV–vis spectra of CoO_x/Al_2O_3 samples of different cobalt loadings and preparation methods.

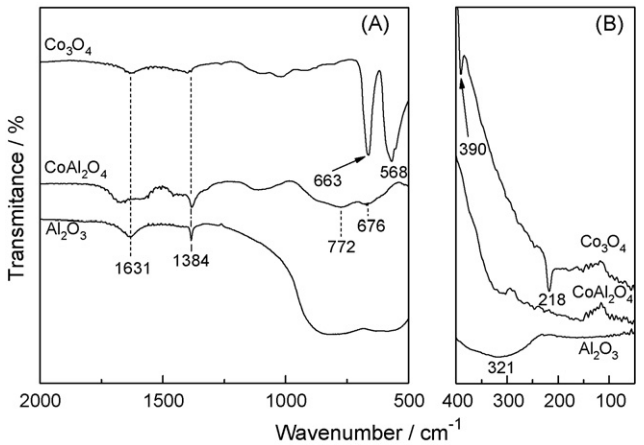

Fig. 4. Infrared (A) and Far-infrared (B) spectra of Co_3O_4; $CoAl_2O_4$ and Al_2O_3.

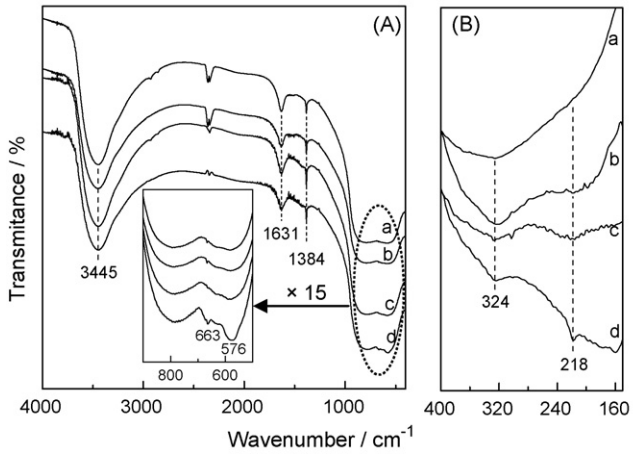

Fig. 5. FT-IR (A) and Far-FT-FIR (B) spectra of Co/γ-Al_2O_3 catalysts with different cobalt loadings: (a) IW1; (b) IW2; (c) IW4 and (d) IW8.

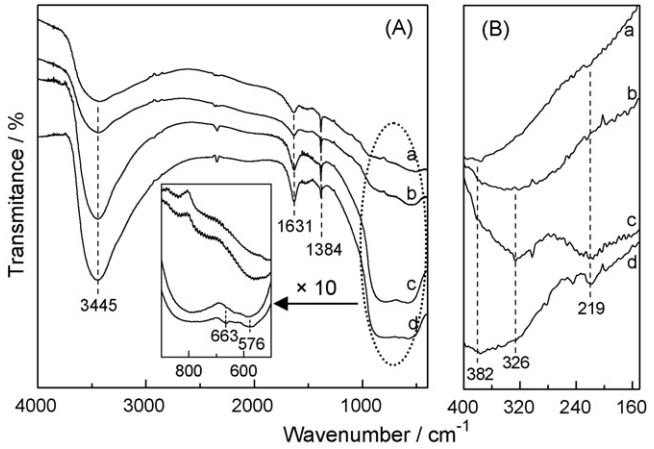

Fig. 6. FT-IR (A) and Far-FT-FIR (B) spectra of Co/γ-Al_2O_3 catalysts synthesized by different methods: (a) sol–gel; (b) co-precipitate; (c) incipient wetness impregnation and (d) solid dispersion.

Fig. 5 shows the IR (A) and Far-IR (B) spectra of CoO_x/Al_2O_3 catalysts with different cobalt loading. A band at 3445 cm^{-1} assignable to the stretching vibration of surface hydroxyl groups, a water bending band at 1630 cm^{-1}, double bands at 2342 cm^{-1} and 2359 cm^{-1} characteristic of surface carbon dioxide, and a surface carbonation vibration mode at 1383 cm^{-1} are observed in all spectra. Identical to the spectrum of pure alumina, only two broad humps between 900 cm^{-1} and 500 cm^{-1} and a broad band at 324 cm^{-1} are observed in the IR and Far-IR spectra of IW1. This suggests that cobalt species are highly dispersed on the support surface and there is no Co_3O_4 formed in the catalysts with low cobalt loading. However, in the IR spectra of IW4 and IW8, double bands at 663 cm^{-1} and 578 cm^{-1} assignable to Co–O bond vibrations of cubic spinel Co_3O_4 are observed. Furthermore, a band at 218 cm^{-1} characteristic of Co_3O_4 is also observed in the Far-IR spectra of IW4 and IW8. These results suggest that Co_3O_4 is formed in these two catalysts. The formation of Co_3O_4 in CoO_x/Al_2O_3 with high cobalt loading is in good agreement with the results of XRD and UV–vis spectroscopy in this work and the results of ESCA and SIMS characterization of Co/Al_2O_3 reported by Chin and Hercules [39]. Note that the intensities of the bands characteristic of Co_3O_4 increased with the increase of cobalt loading and the same catalyst preparation method. The formation of Co_3O_4 in CoO_x/Al_2O_3 catalysts is obviously enhanced by the increase of their cobalt loading.

Fig. 6 shows the IR (A) and Far-IR (B) spectra of 4 mol% CoO_x/Al_2O_3 catalysts prepared by different methods. As discussed above, the band at 3445 cm^{-1}, 1630 cm^{-1}, double bands at 2342 cm^{-1} and 2359 cm^{-1} and the band at 1383 cm^{-1} characteristic of adsorbed hydroxyl groups O–H, surface water, adsorbed carbon dioxide and surface carbonate are observed in the IR spectra of all samples. In the region of 900–500 cm^{-1} (Fig. 6A), double bands at 663 cm^{-1} and 578 cm^{-1} corresponding to the metal–oxygen vibration in cubic spinel Co_3O_4 are observed in the spectra of SD4 and IW4. However, these two bands are not observed in the spectra of CP4 and SG4. In addition, the band at 219 cm^{-1} characteristic of Co_3O_4 is observed in the spectra of SD4 and IW4 but not in the spectra of CP4 and SG4 (Fig. 6B). These results indicate that the cubic spinel Co_3O_4 species is formed in SD4 and IW4 only.

3.1.4. ESR spectroscopy

Figs. 7 and 8 show the ESR spectra of chosen CoO_x/Al_2O_3 catalysts studied in this work. Unexpectedly, the alumina support shows signals due to paramagnetic impurities. The narrow signal at $g_{eff} \approx 4.16$ could be due to iron (Fe^{3+}) impurities. However, we put our emphasis on the signals only due to cobalt species in the following discussion. The most pronounced cobalt ESR signal present in all samples shown in Figs. 7 and 8 is the absorption at around $g_{eff} \approx 5.20$. This signal varies in intensity for the different catalysts. In principle, cobalt ESR signals in such a system can be due to Co^{2+} in tetrahedral (T_d) or octahedral (O_h) environment. According to theory and literature, however, the signal at $g_{eff} \approx 5.20$ can be explained by Co^{2+} in tetrahedral coordination only. This corresponds well to the observation that only Co^{2+} in T_d position is stable against oxidation. Note that the presented cobalt catalysts are calcined under oxidative conditions. The g_{eff} value observed is in good

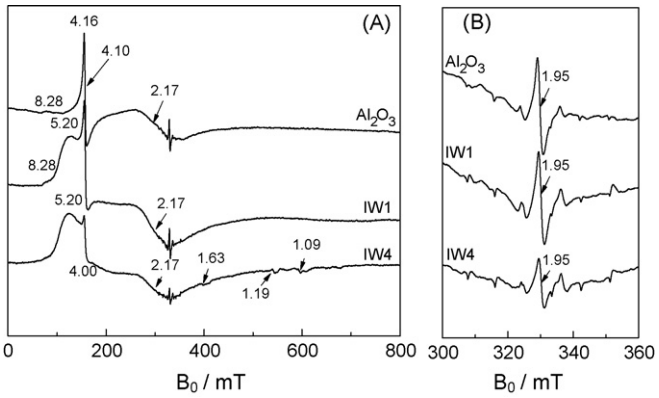

Fig. 7. X-band ESR spectra (T = 130 K) of Co/Al_2O_3 catalysts with different cobalt loadings: IW1: 1 mol% of Co supported on Al_2O_3 and IW4: 4 mol% Co supported on Al_2O_3.

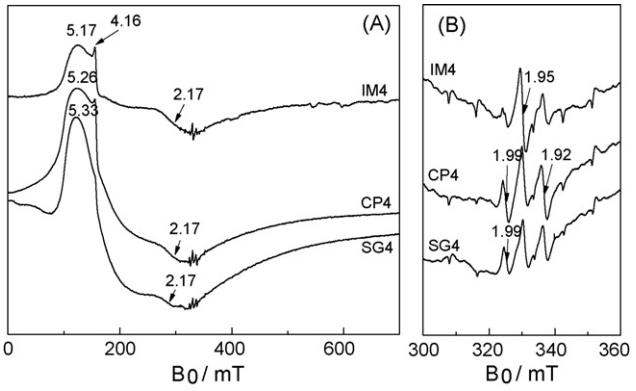

Fig. 8. X-band ESR spectra (T = 130 K) of 4 mol% Co/Al_2O_3 catalysts synthesized by different methods: IW4: incipient wetness impregnation; CP4: co-precipitation and SG4: sol–gel method.

agreement with literature data of $CoCl_4^{2-}$ in T_d coordination (e.g., in an AgCl matrix) [40]. Accordingly we assign this ESR signal to tetrahedral Co^{2+}.

It is interesting to consider the relative intensity of the Co^{2+} (T_d) signal for the catalysts IW4, CP4 and SG4 (Fig. 8). It is obvious that the latter two samples with the clearly higher cobalt dispersion exhibit remarkably higher intensity of this ESR signal. It can be concluded that cobalt is mainly present as Co^{2+}/T_d ($CoAl_2O_4$) in CP4 and SG4, whereas in IW4 only small amount of the cobalt is Co^{2+}/T_d as expected for Co_3O_4.

3.2. Catalytic performance of CoO_x/Al_2O_3 in SCR of NO by C_3H_8

Tables 2 and 3 summarize the catalytic performances of Al_2O_3 and CoO_x/Al_2O_3 for the SCR of NO by C_3H_8 as a function of temperature in a fixed bed continuous flow microreactor. The formation of N_2O is found to be negligible in this work because the selectivity of NO to N_2 is higher than 98% in all experiments. The conversion of both NO and C_3H_8 increases with the increase of reaction temperature in the range between 573 K and 723 K. However, the reductant efficiency decreased with the increase of the reaction temperature in the experimental temperature range.

The effect of cobalt loading on the catalytic performance of CoO_x/Al_2O_3 for SCR of NO by C_3H_8 is demonstrated in Table 2. Modification of Al_2O_3 with a small amount of cobalt significantly enhances the NO conversion. Indeed, only 23.1% of NO is reduced on Al_2O_3 at 673 K. The conversion of NO increased to 91% over 0.5 mol% CoO_x/Al_2O_3 (IW05) and 98.8% over 1.0 mol% CoO_x/Al_2O_3 (IW1) at the same reaction temperature. When the cobalt loading is higher than 1 mol%, the NO conversion decreased with the increase of cobalt loading. For example, NO reduction decreased to 91% on IW2 and 40% on IW4 from 98.8% on IW1. These results suggest that there is an optimum value of cobalt loading for NO reduction. In contrast to NO conversion, the conversion of propane continuously increases with the increasing of cobalt (even higher than the optimum value), leading to a decrease of the reductant efficiency.

Table 3 shows the catalytic performances of CoO_x/Al_2O_3 prepared by different methods. The catalysts prepared by co-precipitation (CP4) and sol–gel (SG4) show higher NO conversion (92.8% and 92.1 at 723 K, respectively) than the catalysts prepared by incipient wetness impregnation and solid dispersion (67.4% for IW4 and 42.2 for SD4) at the same reaction temperature. Interestingly, the catalyst prepared by solid dispersion (SD4) shows the poorest NO conversion but

Table 2
Catalytic performance of Al_2O_3 and CoO_x/Al_2O_3 for SCR of NO using C_3H_8

Catalyst	Temperature (K)	X_{NO}[a] (%)	$X_{C_3H_8}$[b] (%)	X_{NO}:$X_{C_3H_8}$	NOCF[c] (%)
Al_2O_3	623	10.1	1.7	5.9	59.4
	673	23.1	6.7	3.4	34.3
	723	55.9	22.0	2.5	25.4
IW05	623	16.7	4.2	4.0	39.8
	673	91.4	29.9	3.1	30.7
	723	100	47.3	2.1	21.1
IW1	623	22.7	8.3	2.7	27.3
	673	98.8	43.2	2.3	22.9
	723	100	60.9	1.6	16.4
IW2	623	23.9	12.2	2.0	19.6
	673	91.2	52.4	1.7	17.4
	723	99.4	84.9	1.2	11.7
IW4	623	9.9	8.2	1.2	12.1
	673	40.0	38.2	1.0	10.5
	723	67.4	85.4	0.8	7.9
IW8	623	0.3	23.7	–	0.1
	673	1.8	63.6	–	0.3
	723	3.1	97.7	–	0.3

[a] NO conversion: $([NO]_{inlet} - [NO]_{outlet})/[NO]_{inlet} \times 100\%$.
[b] C_3H_8 conversion: $([C_3H_8]_{inlet} - [C_3H_8]_{outlet})/[C_3H_8]_{inlet} \times 100\%$.
[c] NO competitiveness factor: $([NO]_{inlet} - [NO]_{outlet})/\{10 \times ([C_3H_8]_{inlet} - [C_3H_8]_{outlet})\} \times 100\%$.

Table 3
Effect of preparation method on the catalytic performances of CoO_x/Al_2O_3 for SCR of NO using C_3H_8

Sample	Temperature (K)	X_{NO}[a] (%)	$X_{C_3H_8}$[b] (%)	X_{NO}:$X_{C_3H_8}$	NOCF[c]
CP4	623	34.9	11.9	2.9	29.3
	673	89.9	41.9	2.1	21.4
	723	92.8	72.6	1.3	12.8
SG4	623	24.7	11.3	2.2	21.8
	673	78.3	43.4	1.8	18.0
	723	92.1	80.7	1.1	11.4
IW4	623	9.9	8.2	1.2	12.1
	673	40.0	38.2	1.0	10.5
	723	67.4	85.4	0.8	7.9
SD4	623	6.5	10.3	0.6	6.3
	673	28.5	54.0	0.5	5.3
	723	42.2	86.7	0.5	4.9

[a] NO conversion: $([NO]_{inlet} - [NO]_{outlet})/[NO]_{inlet} \times 100\%$.
[b] C_3H_8 conversion: $([C_3H_8]_{inlet} - [C_3H_8]_{outlet})/[C_3H_8]_{inlet} \times 100\%$.
[c] NO competitiveness factor: $([NO]_{inlet} - [NO]_{outlet})/\{10 \times ([C_3H_8]_{inlet} - [C_3H_8]_{outlet})\} \times 100\%$.

highest C_3H_8 conversion at 723 K. The worst NO conversion on SD4 may result from the decrease of reductant efficiency, resulting from the enhanced combustion of propane in the presence of Co_3O_4.

3.3. Effect of cobalt loading on the surface properties of CoO_x/Al_2O_3

The dispersion and properties of cobalt in CoO_x/Al_2O_3 vary with the cobalt loading. For catalysts with low cobalt loading (IW05 and IW1 as examples), cobalt species are highly dispersed and adsorbed on the support surface and no Co_3O_4 is formed. This is verified by the absence of Co_3O_4 reflex in XRD patterns (Fig. 1) and the similarity of IR and Far-IR spectra of CoO_x/Al_2O_3 and pure γ-Al_2O_3 (Fig. 5). The UV–vis (Fig. 3) and ESR results (Fig. 7) of IW1 further demonstrate that tetrahedral Co^{2+} is the predominant cobalt species present in this catalyst. The presence of reflexes at 19.2°, 31.4°, 56.1° and 65.7° in the XRD patterns (Fig. 1) and the appearance of the bands at 663 cm^{-1}, 576 cm^{-1} and 218 cm^{-1} in IR and Far-IR spectra (Fig. 5) demonstrate that Co_3O_4 is formed in CoO_x/Al_2O_3 catalysts with high cobalt loading (IW4 and IW8 for instance). The dispersion and the oxidation states of cobalt supported on alumina strongly depend on the precursor of cobalt, synthesis procedure, cobalt loading and calcination temperature. E. Finocchio et al. [41] and Yan et al. [27] reported that $CoAl_2O_4$ was formed in CoO_x/Al_2O_3 calcined at 673 K using cobalt acetate and cobalt citrate as the cobalt precursor. In this work, the formation of $CoAl_2O_3$ at 723 K calcined IW05 and IW1 could be due to the extremely low cobalt loading (0.5 mol% and 1 mol% corresponding 0.3 wt% and 0.6 wt%). Cobalt ions are assumed to be dispersed and adsorbed on alumina surface hydroxyl sites forming isolated centers like [≡Al–O–Co] and/or [(≡Al)$_2$O–Co]. These structures may be precursors for the formation of $CoAl_2O_4$ during thermal treatment. Increase of cobalt concentration results in the conglomeration of cobalt on the alumina surface. Subsequently, the conglomerated cobalt species is decomposed to Co_3O_4 during calcination [18,31].

3.4. Effect of preparation method on cobalt–alumina interactions

The interactions between metal ions and support may effect on the surface properties and thus overall catalytic performance of the catalyst. [18] In this study, the degree of cobalt–alumina interactions was varied by the different preparation methods.

For catalyst CP4, besides the formation of cobalt hydroxide and alumina hydroxide, a so-called mixed metal layer double hydroxide (LDH) is formed during the co-precipitation according to the reaction of

$$x\mathrm{Co}^{2+}{}_{(aq)} + y\mathrm{Al}^{3+}{}_{(aq)} + (2x+3y)\mathrm{OH}^{-}{}_{(aq)} = \mathrm{Co}_x\mathrm{Al}_y(\mathrm{OH})_{(2x+3y)(s)}$$

The formation of cobalt–alumina–LDH during co-precipitation has also been reported by Velu et al. [42] and Zheng and co-workers [43] recently. During the thermal decomposition of these metal hydroxides, the intermediately formed CoO reacts with ''in situ'' generated alumina forming $CoAl_2O_4$. The formation of $CoAl_2O_4$ is revealed by XRD, UV–vis, IR and ESR spectroscopy.

For catalyst SG4, cobalt ions were premixed with the liquid alumina sol and the Al–O–Co bonds are formed during the gelation. The mixing of cobalt and aluminum at atomic level leads to the formation of $CoAl_2O_4$ during the thermal decomposition of the precursor of SG4. However, the formation of CoO (evidenced by the band characteristic of octahedral Co^{2+} in the UV–vis spectra, Fig. 3) suggests that not all $Co(NO_3)_2{\cdot}6H_2O$ is reacted to alumina xerogel. The formation of both $CoAl_2O_4$ and CoO in Co/Al_2O_3 prepared by sol–gel method has also been revealed by Ji et al. [31] using XPS spectroscopy. Because CoO is not formed in CP4, it can be proposed that the mean cobalt–alumina interaction in CP4 is

stronger than that of SG4. Since cobalt ions have penetrated into alumina lattice forming cobalt aluminate, the cobalt–alumina interaction in these catalysts could be the strongest among the catalysts reported in this work.

Cobalt ions can hardly penetrate into the support lattice to form $CoAl_2O_4$ spinel at 723 K because γ-Al_2O_3 is chemically stable. For this reason, γ-Al_2O_3 acts only as a dispersion medium and Co_3O_4 is detected by X-ray diffraction, UV–vis, IR and Far-IR spectroscopy in IW4 and SD4. The observed Co_3O_4 phase is formed by the decomposition of $Co(NO_3)_2{\cdot}6H_2O$, which was introduced onto the surface of γ-Al_2O_3 support by impregnation (IW4) or solid dispersion (SD4). The formation of Co_3O_4 in IW4 and SD4 indicates that there is no chemical reaction between cobalt ions and the support (alumina) in these catalysts. The cobalt–alumina interaction is very weak in these catalysts because cobalt oxides are mechanically mixed with alumina or physically dispersed on alumina surface only.

3.5. Structure–activity relationships in SCR of NO by propane over CoO_x/Al_2O_3

The dispersion and oxidation states differed from the cobalt loading and preparation methods (see above) and can subsequently influence the catalytic performance of CoO_x/Al_2O_3 in the SCR reaction. Yan et al. [27] investigated the effect of cobalt precursor, catalyst preparation method and calcination temperature on the catalytic properties of Co/Al_2O_3 in SCR of NO by C_3H_6. The authors proposed that CoO is the active species for reduction of NO, $CoAl_2O_4$ has been detected in the most active catalysts as well. Hamada et al. [26,29] studied the activity of SCR of NO by C_3H_6 over Co/Al_2O_3 prepared by sol–gel and impregnation methods. The authors suggested that it is $CoAl_2O_4$ that enhanced the activity for SCR-NO reaction. Furthermore, Okazaki et al. [44,45] investigated the roles of $CoAl_2O_4$, Co_3O_4 and alumina for SCR-NO with ethene and proposed that the synergy of $CoAl_2O_4$ and Al_2O_3 particles at their interface is a crucial factor causing the high activity of $CoAl_2O_4$-Al_2O_3 catalysts.

In this work, the impregnation of a small amount of cobalt onto alumina surface significantly improves the NO conversion (Table 2). Note that tetrahedral Co^{2+} is the dominant cobalt species existing in the low cobalt loading catalysts as discussed above (Figs. 1, 3, 5 and 7). It can be concluded that the presence of tetrahedral Co^{2+} in CoO_x/Al_2O_3 with low cobalt loading enhanced the reduction of NO to N_2. A further increase of the cobalt loading leads to a decrease of NO conversion when the cobalt loading is higher than 1 mol%. In contrast to NO conversion, the conversion of propane continuously increases with the increasing of cobalt (even higher than the optimum value), which results in a decrease of the reductant efficiency (Table 2). This suggests that a side reaction (combustion of C_3H_8 by O_2) rather than the reduction of NO by C_3H_8 has been effectively catalyzed by CoO_x/Al_2O_3 catalyst with high cobalt loading. Considering that the formation of Co_3O_4 is enhanced with the increasing of cobalt loading in CoO_x/Al_2O_3 catalysts (as discussed above), we attribute the decrease in NO reduction to the enhancement of C_3H_8 combustion catalyzed by Co_3O_4.

The differences in cobalt–alumina interactions effect on the surface property and thus overall catalytic activity of CoO_x/Al_2O_3 in SCR of NO by C_3H_8 significantly. As shown in Table 3, the activity and reductant efficiency of CP4 and SG4 in SCR of NO by propane are much better than that of IW4 and SD4 at the same reaction temperatures. This corresponds well with the cobalt–alumina interactions discussed above. Due to the correlation of the catalytic performance and structure of CoO_x/Al_2O_3 we propose that surface $CoAl_2O_4$ formed by penetration of cobalt into alumina is the active species for SCR reaction; enhancing cobalt–alumina interactions may improve the reduction of NO to N_2 by propane.

4. Conclusions

A series of Al_2O_3 supported cobalt oxide catalysts has been prepared, characterized and used in the SCR of NO by propane. The surface areas of the catalysts used in this work are similar. The results of XRD, IR, Far-IR and ESR characterizations of the catalysts suggest that tetrahedral Co^{2+} is a predominant cobalt species in catalysts with low cobalt loading and the 4 mol% CoO_x/Al_2O_3 catalysts prepared by sol–gel and co-precipitation; Co_3O_4 clusters or agglomerates are the predominant cobalt species in the high cobalt loading catalysts prepared by incipient wetness impregnation and solid dispersion. The optimized CoO_x/Al_2O_3 catalysts have been found to be active in SCR of NO by C_3H_8. The studies on the effect of cobalt loading and catalyst preparation method on the catalytic performance suggest that highly dispersed tetrahedral Co^{2+} in $CoAl_2O_4$ are responsible for the increased SCR activity; Co_3O_4 catalyzes the combustion of C_3H_8. The SCR activity increases with an increase in the strength of cobalt–alumina interactions in the catalysts.

Acknowledgments

The authors thank the Bayerische Forschungsstiftung for financial support; C.H. He acknowledges the Bayerische Forschungsstiftung for a grant. Dr. H.J. Eberle and Dr. J. Spengler (Consortium für elektrochemische Industrie GmbH) are acknowledged for their fruitful cooperation and useful discussions.

References

[1] M.D. Amiridis, T. Zhang, R.J. Farranto, Appl. Catal. B 10 (1996) 203.
[2] M. Shelef, Chem. Rev. 95 (1995) 209.
[3] M.D. Fokema, J.Y. Ying, Catal. Rev. 43 (2001) 1.
[4] V.I. Parvulescu, P. Grange, B. Delmon, Catal. Today 46 (1998) 233.
[5] A.Z. Ma, M. Muhler, W. Grunert, Appl. Catal. B 27 (2000) 37.
[6] R. Burch, J.P. Breen, C.J. Hill, B. Krutzsch, B. Konrad, E. Jobson, L. Cider, K. Eranen, F. Klingstedt, L.E. Lindfors, Top. Catal. 30–31 (2004) 19.
[7] Y.J. Li, J.N. Armor, Appl. Catal. B 1 (1992) L31.
[8] M. Iwamoto, H. Yahiro, S. Shundo, Y. Yoshihiro, N. Mizuno, Appl. Catal. 69 (1991) L15.
[9] Y. Wang, B.N. Zong, X.H. Bao, M. Muhler, Catal. Lett. 66 (2000) 237.

[10] D.B. Lukyanov, G. Sill, J.L. Ditri, W.K. Hall, J. Catal. 153 (1995) 265.
[11] T. Beutel, B. Adelman, W.M.H. Sachtler, Catal. Lett. 37 (1996) 125.
[12] Z.J. Li, M. Flytzani-Stephanopoulos, J. Catal. 182 (1999) 313.
[13] C. Shi, M.J. Cheng, Z.P. Qu, X.F. Yang, X.H. Bao, Chin. J. Catal. 22 (2001) 555.
[14] Z.R. Ismagilov, R.A. Shkrabina, L.T. Tsykoza, V.A. Sazonov, S.A. Yashnik, V.V. Kuznetsov, N.V. Shikina, H.J. Veringa, Top. Catal. 16 (2001) 307.
[15] Y.K. Park, J.W. Lee, C.W. Lee, S.E. Park, J. Mol. Catal. A 158 (2000) 173.
[16] C. Wogerbauer, M. Maciejewski, A. Baiker, U. Gobel, Top. Catal. 16 (2001) 181.
[17] B.I. Mosqueda-Jimenez, A. Jentys, K. Seshan, J.A. Lercher, J. Catal. 218 (2003) 375.
[18] M.C. Kung, H.H. Kung, Top. Catal. 10 (2000) 21.
[19] C. He, M. Paulus, J. Find, J.A. Nickl, H.-J. Eberle, J. Spengler, W. Chu, K. Koehler, J. Phys. Chem. B 109 (2005) 15906.
[20] J. Li, J. Hao, L. Fu, T. Zhu, Top. Catal. 30 (13) (2004) 81.
[21] N. Okazaki, S. Tsuda, Y. Shiina, A. Tabata, Chem. Lett. (1998) 51.
[22] C. He, K. Koehler, Chem. Phys. Phys. Chem. 8 (2006) 898.
[23] S. Bennici, A. Gervasini, N. Ravasio, F. Zaccheria, J. Phys. Chem. B 107 (2003) 5168.
[24] H. He, C. Zhang, Y. Yu, Catal. Today 90 (2004) 191.
[25] F. Radtke, R.A. Koppel, E.G. Minardi, A. Baiker, J. Catal. 167 (1997) 127.
[26] H. Hamada, Y. Kintaichi, M. Inaba, M. Tabata, T. Yoshinari, H. Tscuchisa, Catal. Today 29 (1996) 53.
[27] J.Y. Yan, M.C. Kung, W.M.H. Sachtler, H.H. Kung, J. Catal. 172 (1997) 178.
[28] T. Horiuchi, T. Fujiwara, L. Chen, K. Suzuki, T. Mori, Catal. Lett. 78 (2002) 319.
[29] H. Hamada, Y. Kintaichi, M. Sasaki, I. Ito, Appl. Catal. 75 (1991) L1.
[30] T. Nanba, A. Uemura, A. Ueno, M. Haneda, H. Hamada, N. Kakuta, H. Miura, H. Ohfune, Y. Udagawa, Bull. Chem. Soc. Jpn. 71 (1998) 2331.
[31] L. Ji, J. Lin, H.C. Zeng, J. Phys. Chem.: B 104 (2000) 1783.
[32] M.L. Jacono, A. Cimino, G.C.A. Schuit, Gazzetta Chim. Ital. 103 (1973) 1281.
[33] G.N. Asmolov, O.V. Krylov, Kinet. Catal. 12 (1971) 403.
[34] L.F. Liotta, G. Pantaleo, A. Macaluso, G.D. Carlo, G. Deganello, Appl. Catal. A 245 (2003) 167.
[35] T. He, D.R. Chen, X.L. Jiao, Chem. Mater. 16 (2004) 737.
[36] H.Y. Guan, C.L. Shao, S.B. Wen, B. Chen, J. Gong, X.H. Yang, Mater. Chem. Phys. 82 (2003) 1002.
[37] U.L. Stangar, B. Orel, J. Sol–Gel Sci. Tech. 26 (2003) 771.
[38] G. Busca, V. Lorenzelli, V.S. Escribano, R. Guidetti, J. Catal. 131 (1991) 167.
[39] R.L. Chin, D.M. Hercules, J. Phys. Chem. 86 (1982) 360.
[40] L. Van Robbroeck, E. Goovaerts, D. Schoemaker, Phys. Stat. Sol.: A 132 (1985) 179.
[41] E. Finocchio, T. Montanari, C. Resini, G. Busca, J. Mol. Catal. A 204–205 (2003) 535.
[42] S. Velu, K. Suzuki, M.P. Kapoor, S. Tomura, F. Ohashi, T. Osaki, Chem. Mater. 12 (2000) 719.
[43] Z.Z. Chen, E.W. Shi, W.J. Li, Y.Q. Zheng, J.Y. Zhuang, B. Xiao, L.A. Tang, Mater. Sci. Eng. B 107 (2004) 217.
[44] N. Okazaki, R. Fujii, A. Tada, J. Jpn. Petrol. Inst. 45 (2002) 237.
[45] N. Okazaki, Y. Yamamoto, H. Itoh, A. Tada, Chem. Lett. (1998) 807.